Interaction of structure-specific and promiscuous G-protein–coupled receptors mediates small-molecule signaling in *Caenorhabditis elegans*

Donha Park[a,1,2], Inish O'Doherty[b,c,3], Rishi K. Somvanshi[d,3], Axel Bethke[b,c], Frank C. Schroeder[b,c,2], Ujendra Kumar[d], and Donald L. Riddle[a]

[a]Michael Smith Laboratories, University of British Columbia, Vancouver, BC, Canada, V6T 1Z4; [b]Boyce Thompson Institute and [c]Department of Chemistry and Chemical Biology, Cornell University, Ithaca, NY 14853; and [d]Faculty of Pharmaceutical Sciences, University of British Columbia, Vancouver, BC, Canada V6T1Z3

Edited by Jerrold Meinwald, Cornell University, Ithaca, NY, and approved May 8, 2012 (received for review February 6, 2012)

A chemically diverse family of small-molecule signals, the ascarosides, control developmental diapause (dauer), olfactory learning, and social behaviors of the nematode model organism, *Caenorhabditis elegans*. The ascarosides act upstream of conserved signaling pathways, including the insulin, TGF-β, serotonin, and guanylyl cyclase pathways; however, the sensory processes underlying ascaroside function are poorly understood. Because ascarosides often are multifunctional and show strongly synergistic effects, characterization of their receptors will be essential for understanding ascaroside biology and may provide insight into molecular mechanisms that produce synergistic outcomes in small-molecule sensing. Based on DAF-8 immunoprecipitation, we here identify two G-protein–coupled receptors, DAF-37 and DAF-38, which cooperatively mediate ascaroside perception. *daf-37* mutants are defective in all responses to ascr#2, one of the most potent dauer-inducing ascarosides, although this mutant responds normally to other ascarosides. In contrast, *daf-38* mutants are partially defective in responses to several different ascarosides. Through cell-specific overexpression, we show that DAF-37 regulates dauer when expressed in ASI neurons and adult behavior when expressed in ASK neurons. Using a photoaffinity-labeled ascr#2 probe and amplified luminescence assays (AlphaScreen), we demonstrate that ascr#2 binds to DAF-37. Photobleaching fluorescent energy transfer assays revealed that DAF-37 and DAF-38 form heterodimers, and we show that heterodimerization strongly increases cAMP inhibition in response to ascr#2. These results suggest that that the ascarosides' intricate signaling properties result in part from the interaction of highly structure-specific G-protein–coupled receptors such as DAF-37 with more promiscuous G-protein–coupled receptors such as DAF-38.

chemosensation | photoaffinity labeling | signal transduction | small-molecule receptor | pheromone signaling

Several different aspects of the life history of the model organism *Caenorhabditis elegans* are under the control of a chemically diverse family of small-molecule signals, the ascarosides. Ascarosides function as regulators of developmental timing (1–4), mate attraction (4, 5), aggregation behavior (6, 7), and olfactory learning (8). Chemically, the ascarosides form a modular library of signaling molecules based on the dideoxysugar ascarylose, which is linked to fatty acid-like side chains of varying lengths and is decorated further with additional building blocks derived from amino acid metabolism and other pathways (Fig. 1) (7).

Ascarosides were first identified as the constituents of the dauer pheromone, a signal controlling entry into and exit from the dauer diapause, an alternate larval stage that is nonfeeding, long-lived, and highly stress resistant. *C. elegans* larvae interrupt normal development and enter the dauer diapause when sensing unfavorable conditions, such as high population density, limited food, high temperature, or microbial pathogenesis (9–11). Formation of dauer larvae requires exposure of the developing L1 larvae to dauer pheromone (12), the most important components of which are the ascarosides ascr#2, ascr#3, ascr#5, and ascr#8 (2–4).

Ascaroside signaling is strikingly complex. More than 100 different ascaroside structures have been identified in *C. elegans*, and there is significant evidence that even small changes is ascaroside structure are associated with strongly altered activity profiles (6, 7). Most ascaroside-mediated phenotypes involve synergistic action of two or more compounds which must be present in specific proportions and concentrations (2–5). Furthermore, individual ascarosides may have more than one function; for example, ascr#3 is involved in dauer formation, male attraction, and hermaphrodite repulsion (2, 5, 6, 13).

Therefore, ascaroside signaling in *C. elegans* constitutes a unique model for the study of small-molecule perception. However, the mechanisms that underlie the diverse, partially overlapping and synergistic activities of the ascarosides are largely unknown. Molecular genetic analysis of dauer-constitutive (Daf-c) and dauer-defective (Daf-d) mutants revealed that dauer pheromone perception is upstream of several conserved pathways, including the *daf-11*/guanylyl cyclase, insulin/IGF, and TGF-β pathways (14–16). These studies suggested that the dauer pheromone signal is detected by G protein coupled receptors (GPCRs) coupled to the *daf-11*/guanylyl cyclase pathway (14).

Recently, the GPCR-encoding *srbc-64* and *srbc-66* genes were shown to participate in ascaroside-mediated dauer induction; however, dauer-inducing activity of ascarosides is abolished only partially in this mutant (17). Subsequently, two functionally redundant GPCR-encoding genes, *srg-36* and *srg-37*, were shown to be required specifically for dauer induction by ascr#5 (18). Here we show that *daf-37* and *daf-38* encode a heterodimeric pair of ascaroside-sensing GPCRs that mediate both dauer formation and behavioral phenotypes. DAF-37 is required specifically for perception of the potent dauer inducer ascr#2, whereas DAF-38 appears to play a cooperative role in the perception of ascr#2 as well as other ascarosides. Using a synthetic photoaffinity-labeled ascr#2 probe, we demonstrate direct binding of ascr#2 to DAF-37. Through cell-specific expression we show that one small molecule. ascr#2, can elicit different phenotypes by binding to the same GPCR (DAF-37) in two different neurons.

Author contributions: D.P., I.O., A.B., F.C.S., and D.L.R. designed research; D.P., I.O., R.K.S., and A.B. performed research; I.O. contributed new reagents/analytic tools; U.K. analyzed data; and D.P., I.O., F.C.S., U.K., and D.L.R. wrote the paper.

The authors declare no conflict of interest.

This article is a PNAS Direct Submission.

[1]Present address: Centre for Molecular Medicine and Therapeutics, Department of Medical Genetics, University of British Columbia, Vancouver, BC, Canada V5Z 4H4.

[2]To whom correspondence may be addressed. E-mail: schroeder@cornell.edu or dpark@cmmt.ubc.ca.

[3]I.O. and R.K.S. contributed equally to this work.

This article contains supporting information online at www.pnas.org/lookup/suppl/doi:10.1073/pnas.1202216109/-/DCSupplemental.

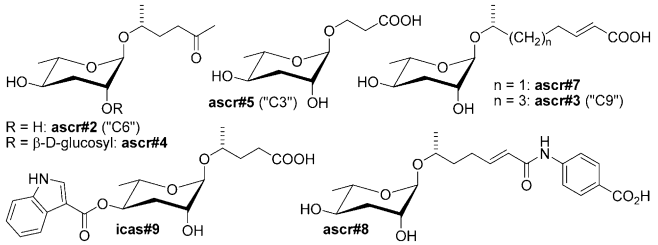

Fig. 1. Ascaroside-based signaling molecules that regulate development and behavior in *C. elegans* (7). Ascr#2, ascr#3, ascr#5, and ascr#8 are dauer pheromone components (2–4), ascr#2, ascr#3, and ascr#8 synergize in male attraction (4, 5); ascr#3 contributes to hermaphrodite repulsion (6, 13); and indole ascarosides (e.g., icas#3) promote hermaphrodite aggregation (6).

Results

GPCRs *daf-37* and *daf-38* Participate in Ascaroside Perception. To identify interacting proteins of the *C. elegans* SMAD DAF-8, a component of TGF-β signaling (19), we immunoprecipitated DAF-8 and analyzed the pulled-down proteins by MS. This approach produced large quantities of DAF-21, a member of the Hsp90 family of molecular chaperones, as well as two previously uncharacterized GPCRs, which we named "DAF-37" and "DAF-38." Their association with components of the TGF-β pathway suggested the possibility that DAF-37 and DAF-38 may partake in dauer pheromone perception. *daf-37* encodes a 465-amino acid GPCR belonging to the serpentine receptor class w family of chemoreceptors in *C. elegans*, one of several chemoreceptor families that have undergone recent expansion in *Caenorhabditis* (Fig. S1) (20). We found that dauer formation in response to ascr#2 was absent or greatly reduced in *daf-37(ttTi3058)* mutants (Fig. 2 *A* and *C*), whereas dauer induction by ascr#3 and ascr#5 in the *daf-37* mutant was similar to that in wild type (Fig. 2*A*) (2). Next we investigated whether *daf-37* is required for ascaroside-induced adult behaviors. Wild-type adult males are attracted to ascr#2, ascr#3, and ascr#8, whereas hermaphrodites are repulsed by all three compounds (5, 13). *daf-37* males were not attracted to ascr#2, but their attraction to ascr#3 or ascr#8 was comparable to that of wild-type males (Fig. 2*E*). As previously reported (4, 5), mixtures of ascr#2 with ascr#3 or ascr#8 showed synergistic male attraction in wild type, but no synergy was detected in the *daf-37* mutant (Fig. 2*E*). *daf-37* hermaphrodites were not repelled by 10 nM of ascr#2, but they responded normally to ascr#3 or ascr#5. Furthermore, equimolar addition of ascr#2 to either ascr#3 or ascr#5 did not show any effect (Fig. S2), indicating that the additive and synergistic effects of ascr#2 are absent in *daf-37* mutants. These results indicate that *daf-37* mutants are defective in larval and adult behaviors mediated specifically by ascr#2.

In contrast, DAF-38, a 465-amino acid GPCR with homology to human gonadotropin-releasing hormone receptor participates in perception of ascr#2 as well as other ascarosides. The two tested *daf-38* alleles formed fewer dauer larvae upon ascr#2 treatment than did wild type; however, dauer induction by ascr#2 was stronger in *daf-38* worms than in *daf-37* worms (Fig. 2 *A* and *B*). In contrast to *daf-37* worms, the *daf-38* mutants also were less responsive to ascr#3 and ascr#5 (Fig. 2*B*). In addition to its Daf-d phenotype, *daf-38* worms exhibited uncoordinated movement and reduced brood size. In genetic epistasis tests, ascr#2-induced dauer formation of *mIs41[daf-37p::cMyc::daf-37]* worms was mostly suppressed by *daf-38* (Table S1), suggesting that genetically *daf-38* acts in parallel or downstream of *daf-37*.

Next, we asked whether overexpression of DAF-37 rescues the strong *daf-37* loss-of-function phenotype. Worms carrying the *mIs41[daf-37p::cMyc::daf-37]* cDNA transgene in a *daf-37*-mutant background showed more than 50% dauer formation even at 1 nM ascr#2, a concentration at which wild-type worms form less

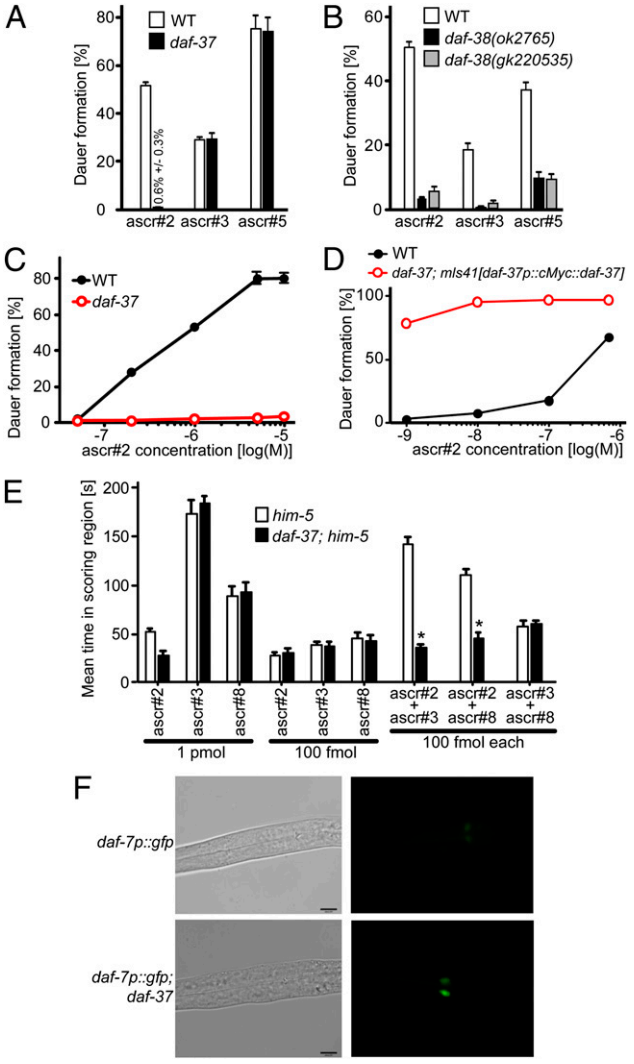

Fig. 2. Ascaroside-dependent phenotypes in *daf-37* and *daf-38* mutant worms. (*A*) Dauer induction by ascr#2 (700 nM), ascr#3 (700 nM), or ascr#5 (500 nM) in wild type and *daf-37* mutants. (*B*) Dauer induction by ascr#2 (700 nM), ascr#3 (700 nM), or ascr#5 (500 nM) in wild type and two *daf-38* mutant alleles. (*C*) Dose–response curve for ascr#2-dependent dauer formation in wild type and *daf-37* mutants. (*D*) Dose–response curve for ascr#2-dependent dauer formation in wild type and *daf-37; mIs41[daf-37p::cMyc::daf-37]* worms. Error bars in *A–D* represent SEM. (*E*) Attraction of *him-5(e1467)* and *daf-37;him-5(e1467)* males to ascarosides. Individual ascarosides or combinations of two ascarosides were used. Error bars represent SEM. $*P < 0.01$, unpaired *t* test, compared with *him-5*. (*F*) Suppression of *daf-7*/TGF-β ligand expression by ascr#2. Transgenic worms carrying *daf-7p::gfp* in the wild type or in *daf-37* background were hatched on 700 nM ascr#2, and GFP expression was observed when the larvae reached L2 stage.

than 3% dauer (Fig. 2*D*). Under favorable conditions, worms overexpressing DAF-37 develop normally and do not form dauers. This result indicates that overexpression of DAF-37 not only rescues the Daf-d phenotype of the *daf-37* mutant but also confers hypersensitive dauer formation in response to ascr#2.

***daf-37* Functions Upstream of Dauer Signaling Pathways.** To test whether the *daf-37* phenotype results from general chemosensory defects as found in sensory cilia mutants, we assessed the chemotaxis and dye-filling phenotypes of this mutant (21). We found that *daf-37* mutants take up the fluorescent dye 1,1′-dioctadecyl-3,3,3′3′-tetramethylindocarbocyanine perchlorate (DiI) normally and that chemotaxis to benzaldehyde was similar to that seen in

wild type (Fig. S3), suggesting that the Daf-d phenotype in *daf-37* is not caused by general sensory or cilial defects.

To confirm the role of *daf-37* in dauer signaling, we generated double mutants between *daf-37* and Daf-c genes in the guanylyl cyclase (14), TGF-β (22), and insulin-signaling pathways (15). The ascr#2 response of the Daf-C mutants (*daf-11*/guanylyl cyclase, *daf-7*/TGF-β, and *daf-2*/IGF) was indistinguishable from that of the corresponding double mutants with *daf-37*, indicating that *daf-11*, *daf-7*, and *daf-2* act downstream *of daf-37* (Table S1). We further found that ascr#2-induced dauer formation in *mIs41 [daf-37p::cMyc::daf-37]* worms was suppressed by the Daf-d mutants *daf-3(mgDf90)*/Smad and *daf-16(m26)*/FOXO. DAF-7/TGF-β is expressed in the ASI chemosensory neurons, and *daf-7* transcription is repressed by dauer pheromone (22, 23). In the *daf-37* mutant, *daf-7p::gfp* expression was not reduced by ascr#2 treatment in the L2 larva but was suppressed almost completely in wild-type larvae (Fig. 2*F*). This result indicates that DAF-37 is required for the sensing of ascr#2 to mediate dauer formation and that *daf-37* functions genetically upstream of *daf-11*/guanylyl cyclase, *daf-7*/TGF-β, and *daf-2*/insulin signaling. To confirm further the role of ciliary sensing, we tested for ascr#2-induced dauer formation in a *daf-10* mutant that encodes intraflagella protein 22 required for ciliogenesis (24). We found that the *daf-10* mutation suppressed ascr#2-induced dauer formation of *mIs41[daf-37p::cMyc::daf-37]* worms, suggesting that DAF-37 functions in sensory cilia (Table S1).

Photoaffinity-Labeled ascr#2 Binds to DAF-37. To determine whether ascr#2 binds directly to DAF-37, we used photoaffinity labeling of DAF-37 expressed in human cell culture (25, 26). Chemical design of an ascr#2-derived photoaffinity-labeling probe was based on previously described methods (4, 27) and incorporates functional groups that enable photo–cross-linking to the receptor and subsequent conjugation with a reporter while preserving the probe's ability to bind to DAF-37. As a photo–cross-linkable unit we chose a trifluorodiazirine, to which we linked a bio-orthogonal terminal alkyne, which can be conjugated to appropriate azide reporters via click chemistry (Fig. 3*A*). This ascr#2 probe retained dauer-inducing activity in both wild-type and *daf-37*-overexpressing worms, although dauer induction was much weaker than with unmodified ascr#2 (Fig. 3*C*), likely because of the bulk of the added moieties.

To demonstrate binding of the ascr#2 probe to DAF-37, we used amplified luminescence assays [AlphaScreen (28)] and DAF-37 expressed in HEK293T cells (Fig. 3*B*). This technique does not require a protein precipitation step after click chemistry (protein precipitation can pose problems for GPCRs because of their generally poor solubility). For our AlphaScreen assay, we used streptavidin-coated donor beads that, to produce a signal, must come within roughly 200 nm of acceptor beads coated in 1D4 antibody (Fig. 3*B*). In preparation for the assay we delivered the ascr#2 probe to HEK293T cells expressing DAF-37 with a C-terminal 1D4-tag. Following photo–cross-linking and click chemistry with a biotinylated azide, any cross-linked ascr#2 probe/DAF-37–1D4 complex should induce colocalization of donor and acceptor beads, resulting in emission of light at 520–620 nm (Fig. 3*B*). As shown in Fig. 3*D*, addition of the ascr#2 probe to *daf-37::1D4*-expressing cells resulted in a significant increase of luminescence compared with control conditions lacking either *daf-37::1D4* or the ascr#2 probe. Cotransfection of *daf-38* did not increase luminescence further. As an additional control, we transfected cells with human rhodopsin, a related class A GPCR (*daf-37* belongs to rhodopsin-like class A GPCRs) that naturally contains a 1D4 epitope. The addition of the ascr#2 probe to rhodopsin-transfected cells resulted in a small increase of light emission compared with nontransfected cells (Fig. 3*D*); however, this increase was significantly lower than observed for cells transfected with *daf-37::1D4*, even though the levels of rhodopsin expression were dramatically higher than

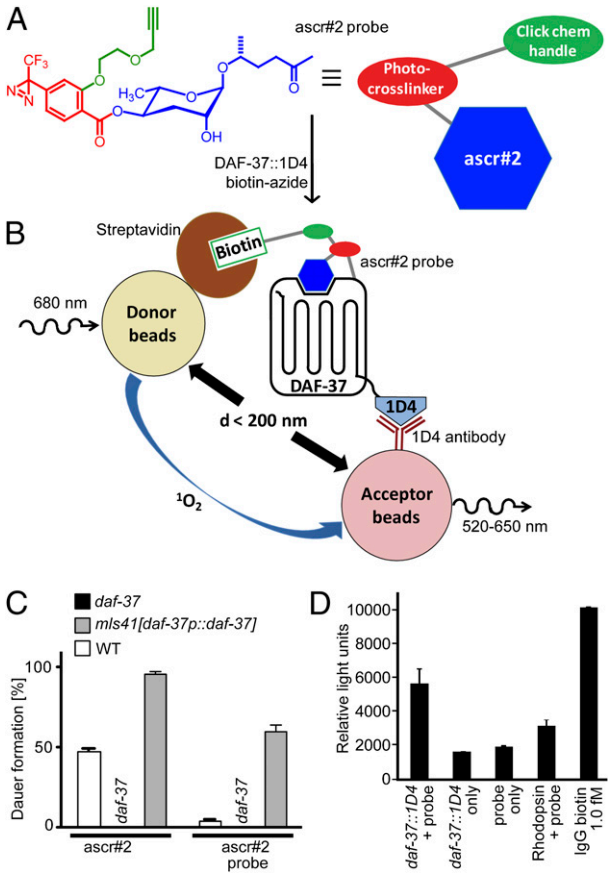

Fig. 3. Photoaffinity-labeled ascr#2 binds to DAF-37. (*A*) Chemical structure of synthetic trifunctional ascr#2 probe, including an ascr#2 moiety (blue), a photosensitive cross-linking unit (red), and an alkyne side chain (green) for click chemistry with biotin azide. (*B*) Schematic representing AlphaScreen of the biotinylated ascr#2 probe covalently bound to DAF-37. Streptavidin-coated donor beads colocalize with 1D4 antibody-coated acceptor beads as a result of the ascr#2 probe's being linked to DAF-37. (*C*) Dauer induction by ascr#2 (500 nM) or ascr#2 probe (500 nM). Error bars represent SEM. (*D*) AlphaScreen shows binding of ascr#2 probe to DAF-37::1D4. Incubation of ascr#2 probe (25 μM) with DAF-37::1D4-expressing cells generates significantly higher luminescence than control experiments without probe, without DAF-37::1D4 transfection, or with cells expressing rhodopsin. See Fig. S4 for a comparison of expression levels of DAF-37::1D4 and rhodopsin. As a positive control, 1 fmol of IgG-biotin was used. Error bars represent SEM.

those of *daf-37* (Fig. S4). These results show that the ascr#2 probe binds specifically to DAF-37.

***daf-37* and *daf-38* Are Expressed in Chemosensory Neurons.** Using transgenic worms expressing dsRED driven by the *daf-37* promoter, we determined that *daf-37* is expressed in the ASI and ASK sensory neurons, in the IL-2 interneurons, and in the male-specific CEM (cephalic sensilla, male) neurons, which are involved in male mating behavior (Fig. 4*A* and Fig. S5*A*) (5, 29). We also generated transgenic worms bearing an N-terminal cMyc translational fusion of *daf-37* cDNA under control of the *daf-37* promoter (*mIs41[daf-37p::cMyc::daf-37]*). Using anti-cMyc antibody, we showed that DAF-37 was localized to the cilia (Fig. S5*B*). A developmental immunoblot showed that DAF-37 is strongly expressed in L1 and L2 stages but is less abundant in the L3, L4, and adult stages. We also detected DAF-37 in dauer larvae, although the level of expression was lower than in any other stages (Fig. S5*C*). These tissue and developmental expression patterns of DAF-37 are consistent with its suggested roles in ascr#2-dependent larval and adult behaviors. Using a *gfp*-reporter

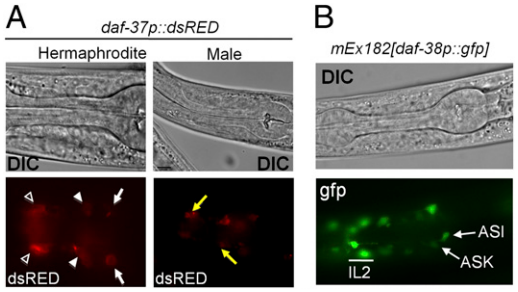

Fig. 4. Expression patterns of *daf-37* and *daf-38*. (*A*) Tissue-specific expression of *daf-37p::dsRED*. DIC and fluorescent images of *daf-37* expression in a hermaphrodite and a male. *daf-37* expression was detected in ASI (arrows), ASK (solid arrowheads), and IL-2 (open arrowheads) neurons as well as in male-specific CEM neurons (*Right*, arrows) (also see Fig. S5). (*B*) DIC and fluorescent images of *daf-38p::gfp* expression in hermaphrodites. *daf-38p::gfp* was detected prominently in the ASI, ASK, and IL-2 neurons and weakly in other head neurons.

construct, we showed that DAF-38 was expressed in the same head neurons as DAF-37 (Fig. 4*B*) but not in any other amphid cells. Their coexpression in the ASI, ASK, and IL-2 neurons suggests that *daf-38* and *daf-37* may have related functions.

Distinct Roles for DAF-37 in ASI and ASK Chemosensory Neurons. The ASI and ASK neurons play major roles in mediating ascaroside-dependent phenotypes. Sensing of dauer pheromone by ASI neurons results in dauer formation (30), whereas ASK neurons mediate ascaroside-induced hermaphrodite repulsion (13). To dissect possible tissue-specific functions of DAF-37, we expressed *daf-37* cDNA under the control of the ASI-specific (*gpa-4*) or ASK-specific (*srbc-64*) promoters in a *daf-37* mutant background (17, 31). ASI-specific expression of *daf-37* not only rescued the *daf-37* Daf-d phenotype but also conferred hypersensitivity to ascr#2 in the dauer formation assay. Dauer formation in the ASK-specific *daf-37* expressor was increased only modestly in comparison with the *daf-37* mutant (Fig. 5*A*). In contrast to the dauer formation phenotype, hermaphrodites expressing *daf-37* in the ASK neurons were hypersensitive to ascr#2 in the repulsion assay, whereas the ASI-specific expressor showed no significant repulsion (Fig. 5*B*). These results suggest that *daf-37* serves

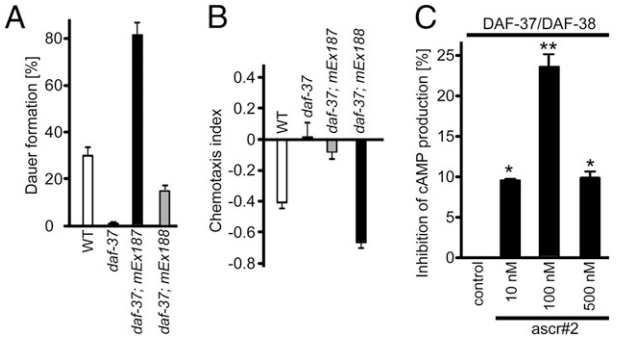

Fig. 5. Rescue of *daf-37* phenotypes by *daf-37* overexpression and tissue-specific roles of DAF-37. (*A*) Dauer induction by ascr#2 in wild type, *daf-37*, *daf-37; mEx187[gpa-4p::daf-37]* (ASI-specific *daf-37*-expression) and *daf-37; mEx188[srbc-64p::daf-37]* (ASK-specific *daf-37*expression). Error bars represent SEM. (*B*) Hermaphrodite repulsion behavior in adult worms in the four strains shown in *A*. Error bars represent SEM. (*C*) Effect of ascr#2 on forskolin-induced cAMP production in HEK293 cells stably transfected with DAF-37 and DAF-38. Data are presented as the percent inhibition of cAMP production in the absence of ascr#2. Error bars represent SE. Data analysis used ANOVA and post hoc Dunnett's test for comparison against basal level. $*P < 0.05$; $**P < 0.01$.

different functions in ASI and ASK neurons: ASI expression regulates dauer formation in larvae, whereas ASK expression regulates hermaphrodite repulsion in adults.

DAF-37 Forms Homodimers and Heterodimers with DAF-38. Many GPCRs form homo- or heterodimers that are required for full function (32). To ascertain whether DAF-37 forms homodimers and/or heterodimers with DAF-38, we used photobleaching fluorescent energy transfer (Pb-FRET) analysis in HEK293 cells. The cells were transfected with cMyc-DAF-37 and/or HA-DAF-38 and were processed for receptor expression by using monoclonal anti-HA and polyclonal anti-cMyc antibodies followed by FITC-conjugated (donor) and Cy3-conjugated (acceptor) secondary antibodies to make donor and acceptor pairs. To determine relative FRET efficiencies, digital photographs were analyzed for photobleaching decay of the donor in the absence or presence of an acceptor in control (Fig. 6*A*) and ascr#2-treated (Fig. 6*B*) conditions. As shown in Table S2, cells monotransfected with DAF-37 displayed a relative Pb-FRET efficiency of 15.4 ± 0.5%, indicating that DAF-37 exists as a homodimer. Upon treatment with ascr#2, the relative Pb-FRET efficiency increased slightly, suggesting agonist-induced stabilization of a receptor complex. HEK293 cells cotransfected with DAF-37/DAF-38 displayed a relative Pb-FRET efficiency of 18.3 ± 0.8%, indicating that the receptors exist as heterodimers. Again, a small but significant increase in relative Pb-FRET efficiency was observed upon ascr#2 treatment. This result suggests that DAF-37 exists as preformed homodimers when expressed alone but preferentially forms heterodimers in cells cotransfected with DAF-37 and DAF-38, and that dimerization is enhanced upon ascr#2 treatment. The specificity of heterodimerization was confirmed in control experiments based on Pb-FRET analysis of cells cotransfected with DAF-37 and rhodopsin or DAF-37 and the chimeric somatostatin receptor SST5CR1, which is incapable of forming dimers. As shown in Fig. S6, relative FRET efficiencies of only 2–3% were observed in both cases, indicating absence of heterodimerization. To demonstrate directly the formation of DAF-37/DAF-38 heterodimers, we performed coimmunoprecipitation using cells cotransfected with cMyc-DAF-37 and HA-DAF-38, which revealed a strong band at 110 kDa indicating formation of DAF-37/DAF-38 heterodimers (Fig. S7). In contrast, control experiments using cells cotransfected with either cMyc-DAF-37/HA-rhodopsin or cMyc-DAF-37/SST5CR1 revealed no evidence for heterodimers (Fig. S7). Last, we investigated whether DAF-37 intracellular localization is affected by DAF-38 coexpression. In monotransfected cells DAF-37 was found in the Golgi apparatus as well as on the plasma membrane. Coexpression of DAF-38 appeared to increase the fraction of membrane-associated DAF-37 slightly (Figs. S8 and S9).

DAF-37/DAF-38 Heterodimerization Is Required for cAMP Inhibition. GPCR homo- and heterodimerization often are associated with signaling changes (33). To investigate the effect of dimerization on DAF-37, we measured DAF-37 receptor function indirectly by coupling to adenyl cyclase. We determined cAMP levels in HEK293 cells monotransfected and cotransfected with DAF-37 and DAF-38. For cAMP estimation, mono-and cotransfected cells were incubated with or without forskolin and in the presence or absence of different concentrations of ascr#2. Only weak inhibition of forskolin-stimulated cAMP levels was observed in monotransfected cells upon treatment with ascr#2. In contrast, DAF-37/DAF-38 cotransfected cells displayed significant inhibition of cAMP levels when treated with 100 nM of ascr#2 (Fig. 5*C*). Higher concentrations of ascr#2 (500 nM) resulted in lower inhibition. These data suggest that presence of both DAF-37 and DAF-38 is required for a fully functional receptor complex.

Discussion

Ascarosides affect nearly every aspect of *C. elegans* life history, and elucidation of the molecular mechanisms of ascaroside

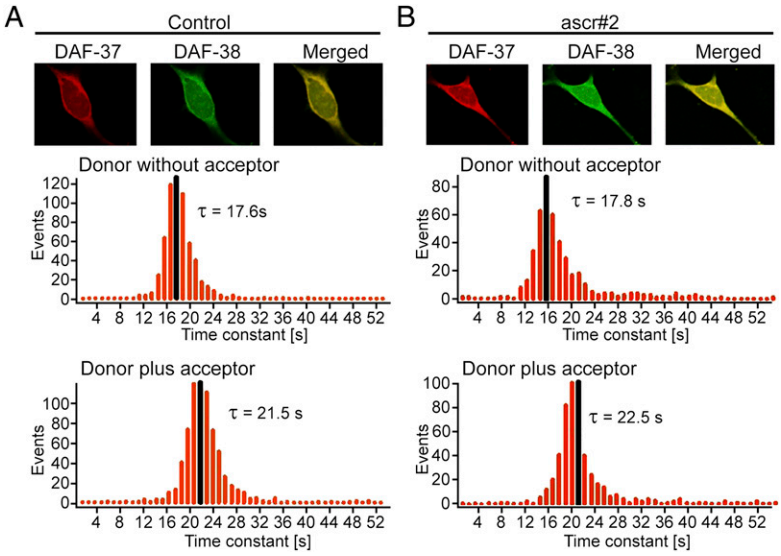

Fig. 6. Microscopic Pb-FRET analysis in HEK293 cells coexpressing DAF-37 and DAF-38 reveals heterodimerization of these two GPCRs. Representative photomicrographs illustrating DAF-37 (red), DAF-38 (green), and colocalization (yellow) in HEK293 cells. Pb-FRET microscopy on control (*A*) and cotransfected HEK293 cells treated with 100 nM ascr#2 (*B*) was performed as described in *Materials and Methods*. Histograms represent pixel-by-pixel analysis of time constant of donor in the absence or presence of acceptor. Gaussian mean time constants (τ) are shown in black. Note the increased time constant (τ) of donor in the presence of acceptor, indicating strong interaction between DAF-37 and DAF-38.

perception will form an important component in advancing the understanding of this model organism's biology. The fact that ascaroside signals consist of mixtures of several different compounds could suggest that each ascaroside is sensed by one or more specific GPCRs. Alternatively, multiple ascarosides may bind to one or several receptors in a (partially) redundant manner. The synergistic effects of different ascarosides in controlling dauer formation (3), male attraction (4, 5), and hermaphrodite repulsion (13) suggested that some specificity for individual ascarosides exists among ascaroside receptors. Our identification of the ascr#2-specific *daf-37* and the recently reported ascr#5-specific *srg-36* and *srg-37* (18) provide examples for highly structure-specific ascaroside receptors. The serpentine receptor class w receptor DAF-37 and the two *srg* genes belong to different families of chemoreceptors, indicating that ascaroside receptors are evolutionarily divergent even though the ascarosides' chemical structures are very similar (20). Our finding that DAF-37 expression in the ASI neurons mediates ascr#2-dependent dauer formation and that expression in the ASK neurons regulates ascr#2-dependent hermaphrodite repulsion demonstrates that perception of one ascaroside by the same receptor expressed in two different neurons can mediate two different phenotypes. Whether *srg-36/37* contribute similarly to ascr#5-dependent hermaphrodite repulsion is unclear but is suggested by the fact that transgenic expression of *srg-36* and *srg-37* in the ASH neurons, where these receptors are not normally expressed, resulted in ascr#5-specific avoidance behavior (18).

Our photoaffinity-labeling studies show that specific recognition of ascr#2 by DAF-37 is associated with direct binding of the ascaroside to this GPCR, whereas direct molecular interactions with ascarosides have not been demonstrated for the *srg-* and *srbc*-family GPCRs. Extension of this labeling approach to other ascarosides may facilitate identification of additional specific receptors. Because of the small size of ascr#2, the attachment of the photosensitive sidechains likely affected the binding properties of the synthesized ascr#2 probe. Many of the more recently identified ascarosides are significantly larger (7) and thus may enable the design of probes with better cross-linking efficacy and identification of binding sites via MS-based proteomics.

The weaker phenotypes of *daf-38* and *srbc-64/66* (17) suggest that other, less specific GPCRs also take part in ascaroside perception. Like *daf-38*, *srbc-64* or *srbc-66* appear to participate in sensing of several different ascarosides, and mutation of *srbc-64* or *srbc-66* only partially affects ascaroside-dependent dauer formation (17). *srbc-64/-66* are further distinguished from *daf-37* and the two *srg-36/37* genes, in that *srbc-64/-66* mutants do not become hypersensitive to ascarosides in response to overexpression of *srbc-64/-66* (17). Furthermore, *srbc-64/-66* mutants are not defective in the ascaroside-mediated behavioral phenotypes.

Our results indicate that DAF-37 is required for specific recognition of ascr#2 and that its heterodimerization with DAF-38 is required to form a functional complex for signal transduction. Many recent studies suggest that GPCRs associate as dimers or even higher-order oligomers (33–35). For example, the GABAB receptor forms a heterodimer in the endoplasmic reticulum and is targeted to the cell surface as a preformed dimer without any agonist-dependent regulation (36). Because *daf-38* is partially required for perception of ascr#2 and several other ascarosides, it is possible that *daf-38*, in addition to *daf-37*, also interacts with receptors specific for other ascarosides. Similarly, *srbc-64/66* may function as parts of receptor GPCR dimers or higher-order oligomers, including more specific receptors such as *daf-37*. Therefore, it appears that the complex signaling properties of the ascarosides may result in part from the interaction of several different types of ascaroside receptors, including highly structure-specific GPCRs that bind directly to ascarosides as well as more promiscuous GPCRs that either bind to several different ascarosides or form heterodimers with several specific ascaroside-binding GPCRs.

Materials and Methods

Details of transgene construction; transformations, cell culture, and transfections; dauer formation, male attraction, and hermaphrodite repulsion; and synthesis and photo–cross-linking of the ascr#2 probe are given in *SI Materials and Methods*.

Nematode Strains. *C. elegans* strains were cultured according to standard techniques (37) unless otherwise noted. Worm strains and alleles used are LG I: *daf-16(m26)*; LG II: *daf-37(ttTi3058)*; LG III: *daf-7(e1372), daf-2(e1370 unc-119(e2498);* LG IV: *daf-38(ok2765), daf-38(gk220535), daf-10(e1387)*; LG V: *daf-11(m47), him-5(e1476)*; LG X: *daf-3(mgDf90). mEx182[daf-38p::gfp, rol-6 (su1006)], Ex184[daf-37p::dsRED, rol-6(su1006)], mEx187[gpa-4p::daf-37, unc-119(+)], mEx188[srbc-64p::daf-37, unc-119(+)], mIs41[daf-37p::daf-37, rol-6(su1006)], otEx2503[gcy-27p::gfp, rol-6(su1006)], otEx2310[gcy-19p::gfp, unc-122::gfp], mIs7[daf-7p::gfp::daf-7 3′UTR], smIs23[pdk-2::gfp], daf-37; him-5, daf-37; unc-119, daf-37; mIs7, daf-37; mIs41, daf-37; daf-38, mIs41; daf-38, daf-38; mIs4, 1mEx182; mEx184, mEx184; otEx2503, mEx184; otEx2310, mEx184; smIs23, mIs41; daf-3, mIs41; daf-16, mIs41; daf-10.*

Ascarosides. Ascarosides were synthesized as described (2, 4). Ascarosides are named using their four-letter small-molecule identifiers (www.smid-db.org).

Pb-FRET Microscopic Analysis. HEK293 cells expressing HA-DAF-38 and/or cMyc-DAF-37 were grown on coverslips to 60–70% confluency and treated with 100 nM ascr#2 for 15 min at 37 °C. Cells were fixed with 4% (wt/vol) paraformaldehyde for 20 min on ice and processed for immunocytochemistry as previously described (38, 39). To create a donor–acceptor pair, monoclonal anti-HA and polyclonal cMyc primary antibodies were used, followed by incubation with FITC- and rhodamine-conjugated secondary antibodies, respectively. The plasma membrane region was used to analyze the photobleaching decay as previously described (38, 39). The FRET efficiency (E) was calculated based upon the photobleaching (Pb) time constants of the donor taken in the absence (D − A) and presence (D + A) of acceptor according to $E = 1 - (D - A/D + A) \times 100$.

Coupling to Adenylyl Cyclase. To determine the receptor coupling to adenylyl cyclase, mono- and cotransfected cells were grown in six-well culture plates (>70% cell confluency) and processed for cAMP assay as described earlier (39). Briefly, cells were incubated with 20 μM forskolin and 0.5 mM 3-isobutyl-1-methylxanthine for 30 min at 37 °C in the presence or absence of different concentrations of ascr#2. Cells then were scraped in 0.1 N HCl, and cAMP was determined by immunoassay using a cAMP kit from BioVision, Inc. (39).

Immunohistochemistry. Antibody staining was performed as previously described (40), using anti-cMyc antibody (ab39688; Abcam) and FITC-labeled goat polyclonal secondary antibody (ab6717; Abcam) to detect cMyc-DAF-37.

Microscopy. A Zeiss Axio Scope equipped with a QImaging camera (RETIGA 2000R) was used for differential interference contrast (DIC) microscopy and dsRed and GFP expression analysis. For DiI staining, cultures were synchronized by hatching purified eggs into M9 buffer that were grown on nutrient broth/glucose agar plates until the L2 stage, washed in M9 buffer (20 mM KH_2PO_4, 42 mM Na_2HPO_4, 8.5 mM NaCl, 1 mM $MgSO_4$), and DiI stained as described (41).

AlphaScreen Assay. Colocalization of the biotinylated ascr#2 probe and 1D4-tagged GPCR (DAF-37) was measured using the PerkinElmer AlphaScreen Mouse IgG detection kit #6760606C (28). Mouse IgG acceptor beads (1.5 μg) were incubated for 30 min on ice with 3 μg 1D4 antibody (http://ubc.flintbox.com) in antibody-binding buffer, followed by centrifugation at 20,000 × *g* for 5 min and washed three times in PBS with 0.1% BSA (wt/vol). Next, 1.5 μg of 1D4 antibody-loaded acceptor beads and 1.5 μg of donor beads were added to the cells such that the final volume was 120 μL. This mixture was incubated for 20 min at room temperature, loaded into three wells of an OPTIplate-384 (PerkinElmer), and assayed in a Bio-Tek Synergy H2 plate reader. Samples were excited by light from a tungsten bulb with a 680/30-nm filter, and luminescence was measured directly afterward with a 570/100-nm filter.

ACKNOWLEDGMENTS. We thank the NemaGENETAG (Nematode Gene-Tagging Tools and Resources) Consortium, Gene Knockout Consortium, *Caenorhabditis* Genetics Center, Don Moerman, and Bob Waterston for strains and Stefan Taubert for helpful discussions. This work was supported by Canadian Institutes of Health Research Grants MOP79458 (to D.L.R.) and MOP10268 and 74465 (to U.K.), National Institutes of Health Grants AG12689 (to D.L.R.) and GM088290 (to F.C.S), and by a grant from the German Science Foundation (to A.B.). I.O. is an O'Reilly Foundation Scholar. U.K. is a Senior Scholar of the Michael Smith Foundation for Health Research.

1. Jeong PY, et al. (2005) Chemical structure and biological activity of the *Caenorhabditis elegans* dauer-inducing pheromone. *Nature* 433:541–545.
2. Butcher RA, Fujita M, Schroeder FC, Clardy J (2007) Small-molecule pheromones that control dauer development in *Caenorhabditis elegans*. *Nat Chem Biol* 3: 420–422.
3. Butcher RA, Ragains JR, Kim E, Clardy J (2008) A potent dauer pheromone component in *Caenorhabditis elegans* that acts synergistically with other components. *Proc Natl Acad Sci USA* 105:14288–14292.
4. Pungaliya C, et al. (2009) A shortcut to identifying small molecule signals that regulate behavior and development in *Caenorhabditis elegans*. *Proc Natl Acad Sci USA* 106:7708–7713.
5. Srinivasan J, et al. (2008) A blend of small molecules regulates both mating and development in *Caenorhabditis elegans*. *Nature* 454:1115–1118.
6. Srinivasan J, et al. (2012) A modular library of small molecule signals regulates social behaviors in *Caenorhabditis elegans*. *PLoS Biol* 10:e1001237.
7. von Reuss SH, et al. (2012) Comparative metabolomics reveals biogenesis of ascarosides, a modular library of small-molecule signals in *C. elegans*. *J Am Chem Soc* 134: 1817–1824.
8. Yamada K, et al. (2010) Olfactory plasticity is regulated by pheromonal signaling in *Caenorhabditis elegans*. *Science* 329:1647–1650.
9. Riddle DL, Albert PS (1997) Genetic and environmental regulation of dauer larva development. *C. elegans II*, eds Riddle DL, Blumenthal T, Meyer BJ, Priess JR (Cold Spring Harbor Laboratory, Cold Spring Harbor, NY), 2nd Ed.
10. Hu PJ (2007) Dauer. *WormBook*, ed the *C. elegans* Research Community, 10.1895/wormbook.1.144.1. Available at http://wormbook.org/chapters/www_dauer/dauer.html. Accessed February 1, 2012.
11. Jensen VL, Simonsen KT, Lee Y-H, Park D, Riddle DL (2010) RNAi screen of DAF-16/FOXO target genes in *C. elegans* links pathogenesis and dauer formation. *PLoS ONE* 5: e15902.
12. Golden JW, Riddle DL (1985) A gene affecting production of the Caenorhabditis elegans dauer-inducing pheromone. *Mol Gen Genet* 198:534–536.
13. Macosko EZ, et al. (2009) A hub-and-spoke circuit drives pheromone attraction and social behaviour in *C. elegans*. *Nature* 458:1171–1175.
14. Birnby DA, et al. (2000) A transmembrane guanylyl cyclase (DAF-11) and Hsp90 (DAF-21) regulate a common set of chemosensory behaviors in *caenorhabditis elegans*. *Genetics* 155:85–104.
15. Kimura KD, Tissenbaum HA, Liu Y, Ruvkun G (1997) daf-2, an insulin receptor-like gene that regulates longevity and diapause in *Caenorhabditis elegans*. *Science* 277: 942–946.
16. Riddle DL, Swanson MM, Albert PS (1981) Interacting genes in nematode dauer larva formation. *Nature* 290:668–671.
17. Kim K, et al. (2009) Two chemoreceptors mediate developmental effects of dauer pheromone in *C. elegans*. *Science* 326:994–998.
18. McGrath PT, et al. (2011) Parallel evolution of domesticated Caenorhabditis species targets pheromone receptor genes. *Nature* 477:321–325.
19. Park D, Estevez A, Riddle DL (2010) Antagonistic Smad transcription factors control the dauer/non-dauer switch in *C. elegans*. *Development* 137:477–485.
20. Thomas JH, Robertson HM (2008) The Caenorhabditis chemoreceptor gene families. *BMC Biol* 6:42.
21. Starich TA, et al. (1995) Mutations affecting the chemosensory neurons of *Caenorhabditis elegans*. *Genetics* 139:171–188.
22. Ren P, et al. (1996) Control of *C. elegans* larval development by neuronal expression of a TGF-beta homolog. *Science* 274:1389–1391.
23. Schackwitz WS, Inoue T, Thomas JH (1996) Chemosensory neurons function in parallel to mediate a pheromone response in *C. elegans*. *Neuron* 17:719–728.
24. Bell LR, Stone S, Yochem J, Shaw JE, Herman RK (2006) The molecular identities of the *Caenorhabditis elegans* intraflagellar transport genes dyf-6, daf-10 and osm-1. *Genetics* 173:1275–1286.
25. Hashimoto M, Hatanaka Y (2008) Recent progress in diazirine-based photoaffinity labeling. *Eur J Org Chem* 2008:2513–2523.
26. Grunbeck A, Huber T, Sachdev P, Sakmar TP (2011) Mapping the ligand-binding site on a G protein-coupled receptor (GPCR) using genetically encoded photocrosslinkers. *Biochemistry* 50:3411–3413.
27. Mayer T (2007) Design and synthesis of a tag-free chemical probe for photoaffinity labeling. *Eur J Org Chem* 2007:4711–4720.
28. Ullman EF, et al. (1994) Luminescent oxygen channeling immunoassay: Measurement of particle binding kinetics by chemiluminescence. *Proc Natl Acad Sci USA* 91: 5426–5430.
29. White JQ, et al. (2007) The sensory circuitry for sexual attraction in *C. elegans* males. *Curr Biol* 17:1847–1857.
30. Bargmann CI, Horvitz HR (1991) Control of larval development by chemosensory neurons in *Caenorhabditis elegans*. *Science* 251:1243–1246.
31. Jansen G, et al. (1999) The complete family of genes encoding G proteins of *Caenorhabditis elegans*. *Nat Genet* 21:414–419.
32. Bulenger S, Marullo S, Bouvier M (2005) Emerging role of homo- and heterodimerization in G-protein-coupled receptor biosynthesis and maturation. *Trends Pharmacol Sci* 26:131–137.
33. Bai M (2004) Dimerization of G-protein-coupled receptors: Roles in signal transduction. *Cell Signal* 16:175–186.
34. Terrillon S, Bouvier M (2004) Roles of G-protein-coupled receptor dimerization. *EMBO Rep* 5:30–34.
35. Milligan G (2010) The role of dimerisation in the cellular trafficking of G-protein-coupled receptors. *Curr Opin Pharmacol* 10:23–29.
36. White JH, et al. (1998) Heterodimerization is required for the formation of a functional GABA(B) receptor. *Nature* 396:679–682.
37. Brenner S (1974) The genetics of *Caenorhabditis elegans*. *Genetics* 77:71–94.
38. Grant M, Patel RC, Kumar U (2004) The role of subtype-specific ligand binding and the C-tail domain in dimer formation of human somatostatin receptors. *J Biol Chem* 279: 38636–38643.
39. Somvanshi RK, Billova S, Kharmate G, Rajput PS, Kumar U (2009) C-tail mediated modulation of somatostatin receptor type-4 homo- and heterodimerizations and signaling. *Cell Signal* 21:1396–1414.
40. Finney M, Ruvkun G (1990) The unc-86 gene product couples cell lineage and cell identity in *C. elegans*. *Cell* 63:895–905.
41. Blacque OE, et al. (2004) Loss of *C. elegans* BBS-7 and BBS-8 protein function results in cilia defects and compromised intraflagellar transport. *Genes Dev* 18: 1630–1642.